### Beach Change Induced by Tropical Storm Eta 2020

Article · June 2021

CITATIONS READS

0 457

1 author:

| Jun Cheng | Kean University | 32 PUBLICATIONS 341 CITATIONS |
| SEE PROFILE |

Some of the authors of this publication are also working on these related projects:

| Project | ship induced wave measurement View project

# Factors controlling longshore variations of beach changes induced by Tropical Storm Eta (2020) along Pinellas County beaches, west-central Florida

By

### Jun Cheng,\* Francesca Toledo Cossu, and Ping Wang

School of Geosciences, University of South Florida, Tampa, FL 33620, USA \*Corresponding author, jun@mail.usf.edu

### **ABSTRACT**

Tropical Storm Eta impacted the coast of west-central Florida from 11 November to 12 November 2020 and generated high waves over elevated water levels for over 20 hours. A total of 148 beach and nearshore profiles, spaced about 300 m (984 ft) apart, were surveyed one to two weeks before and one to eight days after the storm to examine the beach changes along four barrier islands, including Sand Key, Treasure Island, Long Key, and Mullet Key. The high storm waves superimposed on elevated water level reached the toe of dunes or seawalls and caused dune erosion and overwash at various places. Throughout most of the coast, the dune, dry beach, and nearshore area was eroded and most of the sediment was deposited on the seaward slope of the nearshore bar, resulting in a roughly conserved sand volume above closure depth. The longshore variation of beach-profile volume loss demonstrates an overall southward decreasing trend, mainly due to a southward decreasing nearshore wave height as controlled by offshore bathymetry and shoreline configurations. The Storm Erosion Index (SEI) developed by Miller and Livermont (2008) captured the longshore variation of beach-profile volume loss reasonably well. The longshore variation of breaking wave height is the dominant factor controlling the longshore changes of SEI and beach erosion. Temporal variation of water level also played a significant role, while beach berm elevation was a minor factor. Although wider beaches tended to experience more volume loss from TS Eta due to the availability of sediment, they were effective in protecting the back beach and dune area from erosion. On the other hand, smaller profile-volume loss from narrow beach did not necessarily relate to less dune/ structure damage. The opposite is often true. Accurate evaluation of a storm's severity in terms of erosion potential would benefit beach management especially under the circumstance of increasing storm activities due to climate change.

I torms can cause tremendous destruction in coastal regions, such as substantial beach and dune erosion, coastal infrastructure damages, and human life losses. Due to accelerated global sea level rise and increasing frequency and intensity of storms (Griggs and Patsch 2019), coastal communities are expected to become more vulnerable in the near future. Along the U.S. Gulf Coast, many low-lying beaches associated with barrier islands are highly susceptible to extreme storm impacts (Jose et al. 2019; Wang et al. 2020). For the State of Florida, beaches and dunes are especially important in term of social economics as well as natural habitats (Houston 2018). There exists an urgent need to comprehensively and accurately assess a storm's severity in terms of its erosion potential.

In general, storm-induced beach and dune erosion is controlled by two

categories of factors. The first category is associated with the property of the storm (i.e. the driving mechanism). Typical storm factors include the center pressure and wind speed, the size and movement speed of the entire system, and the storm track. These factors determine the heights of storm waves and storm surge, the aerial extent of storm impact, and its duration. The second category relates to the responding environment - beach and dune, in this case. Typical beach and dune factors include: 1) general geological setting that controls the shoreline orientation, sediment size, and rock outcrop in the vicinity of shoreline; 2) width and height of the beach; 3) width, height, and continuity of the dune field; 4) presence or absence of nearshore sandbar; and 5) characteristics of nearshore and offshore bathymetry. These factors control not only how the beach and dune respond **KEYWORDS:** Storm Erosion Index, nearshore sediment transport, beach erosion, coastal sustainability.

Manuscript submitted 28 February 2021; revised & accepted 18 April 2021.

to storm impact but also how the storm forcing (e.g. waves and surge) behaves in the vicinity of the shoreline.

The most broadly used classification for tropical storms is the Saffir-Simpson scale (Saffir 1977; Simpson 1971), which ranks hurricanes into five categories, in addition to a tropical storm category and a tropical depression category. The Saffir-Simpson scale only considers one meteorological characteristic of the storm, namely the center pressure which is closely related to the maximum wind speed. Because most of the stormbeach factors as discussed above are not considered in the Saffir-Simpson scale, its application in assessing beach-dune impact is quite limited and can only provide a very general correlation. Sallenger (2000) developed a storm impact scale specifically for barrier-island coast by evaluating peak storm surge level relative to two elevations describing dune morphology (i.e. the dune toe and dune crest). The Sallenger (2000) scale has been broadly used in both qualitative (Claudino-Sales et al. 2008, 2010; Wang et al. 2006; Wang and Horwitz 2007) and quantitative (Roelvink et al. 2009) assessments of morphologic response of barrier islands to storm impact in the forms of beach erosion, dune erosion, beach/dune overwash, or barrier-island inundation.

The Saffir-Simpson and Sallenger (2000) Scale evaluate the storm strength based on 1-min sustained wind speed (Schott *et al.* 2012), and peak storm surge, respectively. The duration of energetic conditions, which plays an essential role in eroding beach and dune, is not consid-

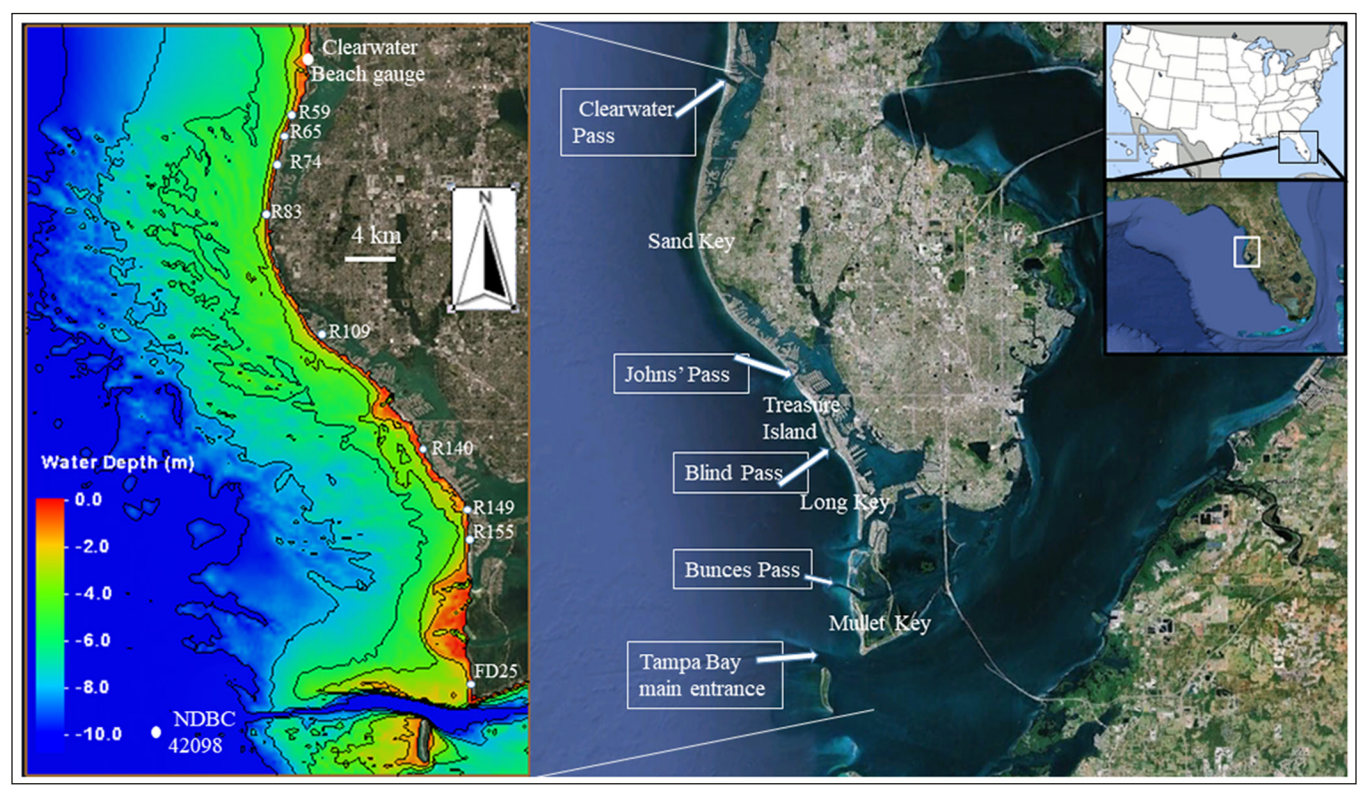


Figure 1. Study area: the beach of Sand Key, Treasure Island, Long Key, and Mullet Key barrier islands along the coast of west-central Florida (map source is Google Earth).

ered by both scales. To more accurately account for storm energy, Miller and Livermont (2008) proposed a Storm Erosion Index (SEI) that includes storm wave and storm surge, as well as storm duration. The SEI has been applied at various locations worldwide — including New Jersey (Lemke and Miller 2020), Gulf of Mexico and Atlantic coast of Florida (Wehof et al. 2014), and Spain (Villatoro et al. 2014) — with the goal of linking beach-volume loss (or shoreline retreat) with the SEI at a spatial scale of tens of kilometers. In this study, we attempt to apply the SEI to interpret spatial variation of beach-dune erosion as caused by Tropical Storm Eta at a scale of several hundred meters (a few thousand feet).

In general, it can be argued that storm factors such as wind, wave and surge are easier to quantify than beach factors through field measurements and numerical modeling. In comparison to storm factors, beach-dune factors typically demonstrate greater spatial variations as controlled by more factors, some of which such as background geological setting cannot be numerically modeled. Therefore, most storm-impact classifications including the three introduced above emphasize storm factors more than beach factors.

Detailed field measurements have demonstrated that storm-induced beachprofile changes along barrier islands are characteristic of substantial spatial variations as influenced by, e.g. the presence or absence of the nearshore sandbars, gentle or steep foreshore slopes, wide or narrow back beaches, etc. These changes in morphologic conditions can occur along a barrier-island coast at a spatial scale of hundreds of meters (a few thousand feet) (Roberts and Wang 2012; Brutsche et al. 2014; Ojeda et al. 2011; Vidal-Ruiz and Ruiz de Alegria-Arzaburu 2019). Since beach nourishment, which has a spatial scale of hundreds to thousands of meters (thousands to tens of thousands of feet), has become a common practice, it would be valuable to investigate the potential of the Miller and Livermont (2008) Storm Erosion Index (SEI) in identifying longshore variations of storm-induced beach-dune erosion at a spatial scale of hundreds of meters. The data collected by this study allows the application of the SEI at a much finer spatial scale, as compared to the previous studies.

The barrier islands of west-central Florida, a low wave-energy coast facing the Gulf of Mexico, experienced the impact of Tropical Storm (TS) Eta in November 2020. The high storm waves superimposed on elevated water level

reached the toes of dunes and impacted various sections of seawall. This study examines the beach morphodynamics associated with this storm event, with the goal of answering the following questions: 1) What are the longshore variations of beach volume changes induced by TS Eta? 2) Can the longshore variations of beach changes be predicted by the Miller and Livermont (2008) SEI? 3) What are the major controlling factors for the longshore variations and are they captured by the SEI? These questions are addressed here based on pre-and post-Eta beachprofiles spaced at 300 m (984 ft) along four barrier islands along the coast of west-central Florida.

### STUDY AREA

The west-central Florida coast is composed of an extensive barrier island chain, including both wave-dominated and mixed-energy barrier islands (Davis and Barnard 2003). Sand Key (Figure 1), the longest barrier island along this coast, is bound to the north by Clearwater Pass and to the south by John's Pass. Both inlets are mixed-energy with relatively large ebb-tidal deltas (Gibeaut and Davis 1993). Complex tidal inlet processes have significant influences on beach morphodynamics at the two ends of the barrier island (Roberts and Wang 2012). The Sand Key barrier island has an overall

shoreline orientation change of 65° from northwest-facing to southwest-facing, controlled by antecedent geology. The stabilized wave-dominated migratory Blind Pass (Wang and Beck 2012) inlet separates Treasure Island to the north and Long Key to the south (Figure 1). Long Key is bound to the south by Pass-A-Grille inlet, which is one of the secondary inlets entering the greater Tampa Bay. Complex tidal inlet processes have significant influences on the adjacent beaches (Beck and Wang 2019). The southmost barrier island studied here, Mullet Key (Figure 1), is bounded to the north by Bunces Pass and to the south by the main entrance (the Egmont Channel) to Tampa Bay.

In order to mitigate the chronic erosion along this coast, beach nourishment projects have been conducted at the beaches along these barrier islands over the past 30 years and have been mostly successful (Davis et al. 2000; Elko and Wang 2007; Roberts and Wang 2012). The northern three barrier islands (Figure 1) are highly developed and densely populated, with hard structures such as Tgroins, jetties, and seawalls in the vicinity of the shoreline. In contrast, Mullet Key, located at the southern end of the study area, is a county park and has relatively little human alterations, although two beach nourishment projects were conducted at the southern end, one in 1973 and one in 2006 (Sandoval 2015; Westfall 2018). Mullet Key is a hook-shaped barrier island situated just to the north of the mouth of Tampa Bay, with one side facing the Gulf of Mexico and the other side facing the Tampa Bay main channel (Figure 1). As Mullet Key is directly landward of the large Tampa Bay ebb tidal delta, the slope of the offshore region is considerably gentler than those of barrier islands to the north.

Along the four studied barrier islands, offshore sand ridges, ebb-tidal deltas, and ancient ebb-tidal deltas from closed inlets introduce bathymetry variations of the inner continental shelf (Figure 1 left panel). The configuration of the shoreline, particularly the presence of the broad headland, and the offshore bathymetry can cause a significant longshore variation of incident wave height and angle (Cheng and Wang 2018; Wang *et al.* 2020). As discussed in the following, the SEI is a strong function of wave height, therefore, in order to accurately assess

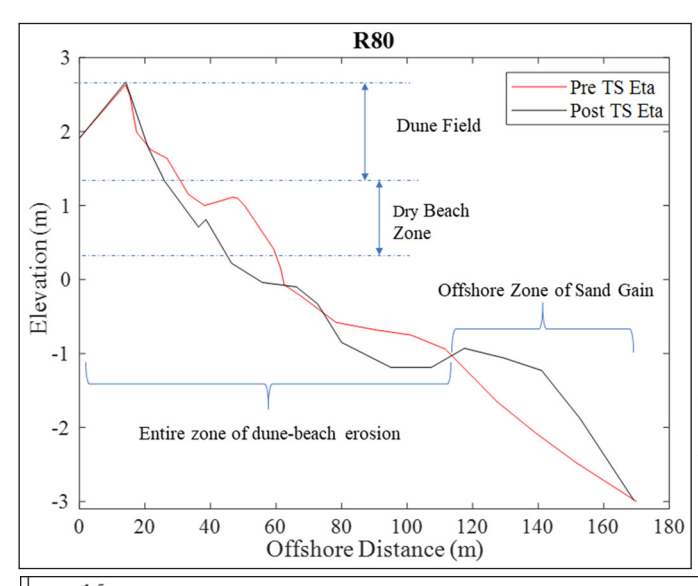


Figure 2. An example beach profile illustrating the four cross-shore zones over which beach-profile volume changes were calculated.

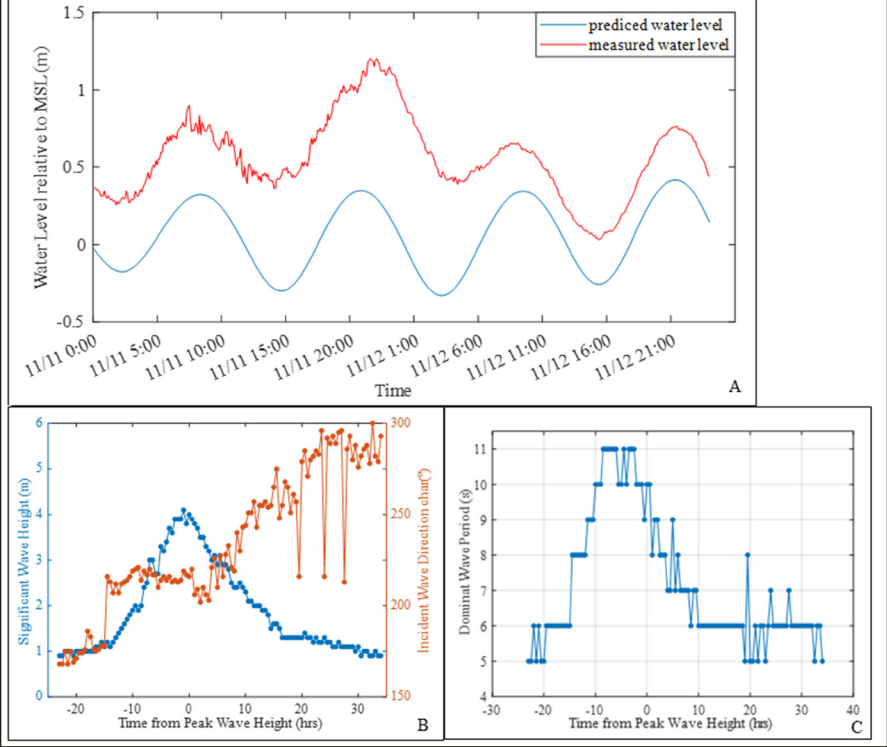


Figure 3. Measured wave and tide conditions associated with the passage of TS Eta: A) predicted and measured water level illustrating the storm surge generated by TS Eta; B) significant wave height and dominant wave direction; and C) dominant wave period.

the erosion potential of a storm, longshore wave-height variations should be captured with adequate spatial resolution.

The west-central Florida coast is a low energy environment with a tidal range of less than 1.2 m and averaged nearshore wave height of less than 0.3 m (Wang and Beck 2012). Waves are typically sea type generated by local winds. Higher waves are often associated with the passages of cold fronts every couple of weeks during the winter and occasional passages of tropical storms in the summer. The sum-

mer season is characterized by typically small waves except during rare passages of a tropical storm. Most tropical storm impacts during the study period were associated with proximal passages of the storm as it moved across the Gulf of Mexico. Prior to TS Eta, the last two proximal passages of tropical storms included Hurricane Hermine in September 2016, and Hurricane Irma in September 2017 (Cheng and Wang 2019). Sediments along the west-central Florida coast are bimodal, composed of siliciclastic and carbonate fractions. The siliciclastic com-

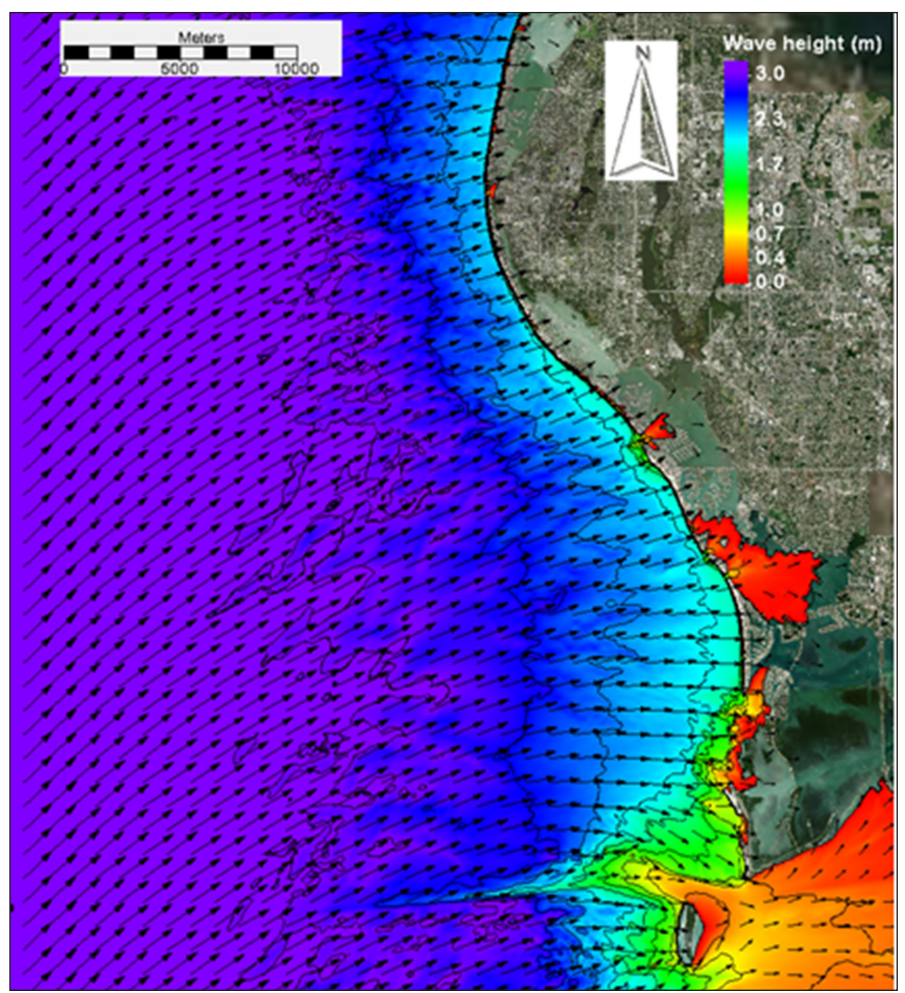


Figure 4. Wave field during the peak of TS Eta as simulated by CMS-Wave, with an input wave height of 4 m at the seaward boundary.

ponent is primarily fine quartz sand with a mean grain size of roughly 0.16 mm. The carbonate fraction is mostly shell debris of various sizes. Mean grain size in the study area varies typically from 0.15 mm to 1.0 mm, controlled by the varying amounts of shell debris.

### **METHODS AND MATERIALS**

This study involved pre- and poststorm beach profile surveys and numerical modeling of wave field associated with TS Eta. The Storm Erosion Index (SEI) developed by Miller and Livermont (2008) was applied to assess longshore variation of beach erosion. In the following, the field and modeling methods are discussed.

#### Beach profile survey and analysis

Beach-profile surveys were conducted from 23 October to 8 November 2020, or less than two weeks before the storm, and from 13 November to 20 November 2020, or one week after the storm. A total of 148 beach profiles were surveyed along the coast, spaced approximately 300 m (984 ft) apart in the longshore direction at the R-monuments established by the State of Florida. The survey lines roughly extended across shore to the short-term closure depth, approximately at -3 m NAVD88 in this area (Wang and Davis 1999). This closure depth has held reasonably well during the passage of TS Eta, as well as during several previous similar storms such as Hurricane Hermine in 2016 and Tropical Storm Debby in 2012, as indicated by the converging pre- and post-storm beach profiles near the seaward end of the survey. The 148 beach profiles span along the four barrier islands, including Sand Key (R55-R124), Treasure Island (JP1, R127-R143), and Long Key (LK1B-LK6, R160-R165), and Mullet Key (FD1-FD 28).

It is important to quantify and understand storm-induced changes in different parts of a dune-beach-sandbar system. Beach-profile volume changes caused by TS Eta were calculated using the Regional Morphology Analysis Package (RMAP) developed by the U.S. Army Corps of

Engineers. Beach-profile volume changes were computed over four zones across the shore, as illustrated in Figure 2, using profile R80 as an example. The four zones are as follows:

- 1) The dune field volume change is represented by that above 1.3 m (4.3 ft) NAVD88 elevation. The seaward edge of the dune field as identified based on vegetation demonstrates some longshore variation. It is acknowledged here that the arbitrary 1.3 m (4.3 ft) elevation may deviate slightly from the dune edge at some locations.
- 2) The dry beach zone is defined here as that between 0.3 m (1.0ft), or roughly the high tide level, and 1.3 m (4.3 ft) NAVD88 (Figure 2). This is the part of the beach that typically draws most public attention and is therefore of particular interest to coastal managers.
- 3) The entire zone of dune-beachnearshore erosion is defined from the landward survey limit (in the dune field or on the seawall where dunes are absent) to the nearshore location where the preand post-storm profiles crossed each other. In the case of profile R80, overall sand volume loss (including sand loss from the dune, the dry beach and the nearshore) was calculated as the changes landward of approximately 110 m (361 ft) distance, where erosion mostly occurred (Figure 2).
- 4) Offshore zone of sand gain is defined from the nearshore location where the pre- and post-storm profiles crossed each other to the short-term closure depth. In the case of the example profile R80, volume gain over the sandbar was calculated as the changes seaward of 110 m (361 ft), where accumulation mostly occurred.

### Wave modeling

In order to investigate the cause of longshore variations of beach erosion/accretion, the nearshore wave fields during the storm conditions were simulated using the CMS-WAVE model (Lin et al. 2011). The CMS-WAVE model has been calibrated and applied in the greater study area (Wang and Beck 2012; Beck et al. 2020). A rather fine resolution of the numerical model grid of 10 m ×10 m (33 X 33 ft) was used to ensure accurate representation of nearshore wave conditions. The bathymetry data of ebb tidal deltas and seaward of the short-term closure

depth to approximately 1 km (0.62 mi) from the shoreline were collected by this study using a ship-mounted single-beam echo sounder synchronized with an RTK-GPS. The pre-Eta beach profiles were used to represent the bathymetry landward of the short-term closure depth. The wave measured by a NDBC gauge at station 42098 (Figure 1 left panel) was used as input offshore boundary condition. The computed wave heights were extracted at 38 selected beach-profile locations at seaward slope of the nearshore sandbar to represent the breaking wave height ( $H_b$ ).

In order to determine the duration of the storm, the 95th percentile of a timeseries of significant wave heights or the 99.9th percentile of water level was used as a threshold value for storm events. The same statistical values were suggested by Lemke and Miller (2020). To avoid missing the duration of the storm with low wave but high surge, or high wave but low surge, the longer duration determined by the threshold values of wave and tide was adopted as suggested by Lemke and Miller (2020). A sufficiently long record is necessary for the computation of the 95th percentile of wave height and 99.9th percentile of water level. As the NDBC wave gauge station #42098 was operational for only a few years, the computed waves extracted from the WAVEWATCH III model at the same location as the NDBC for a 14-year period from 2005 to 2019 was used. The 95th percentile of the wave height of the time-series of WAVEWATCH III data is 1.7 m (5.6 ft). Cheng and Wang (2018) found that the modeled wave height is on average 1.2 times lower than the measured wave height, the 95th percentile wave height of 1.7 m (5.6 ft) was therefore multiplied by 1.2. Thus, a threshold of 2 m (6.6 ft) wave height is determined as the threshold for storm waves. Based on the 2 m (6.6 ft) wave height threshold, the duration of TS Eta was 20 hours. However, based on the computation of 99.9th percentile of measured water level at NOAA Clearwater Beach tide station (Figure 1 left panel) from 2006 to 2019, the threshold value of water level is 0.87 m (2.9 ft), which results in a storm duration of 6.5 hours. Thus, the longer storm duration of 20 hours based on the 95th percentile of wave height is used in this study for the calculation of SEI. It is worth noting that the 2-m (6.6ft) wave height threshold was applied at the offshore boundary of the wave model,

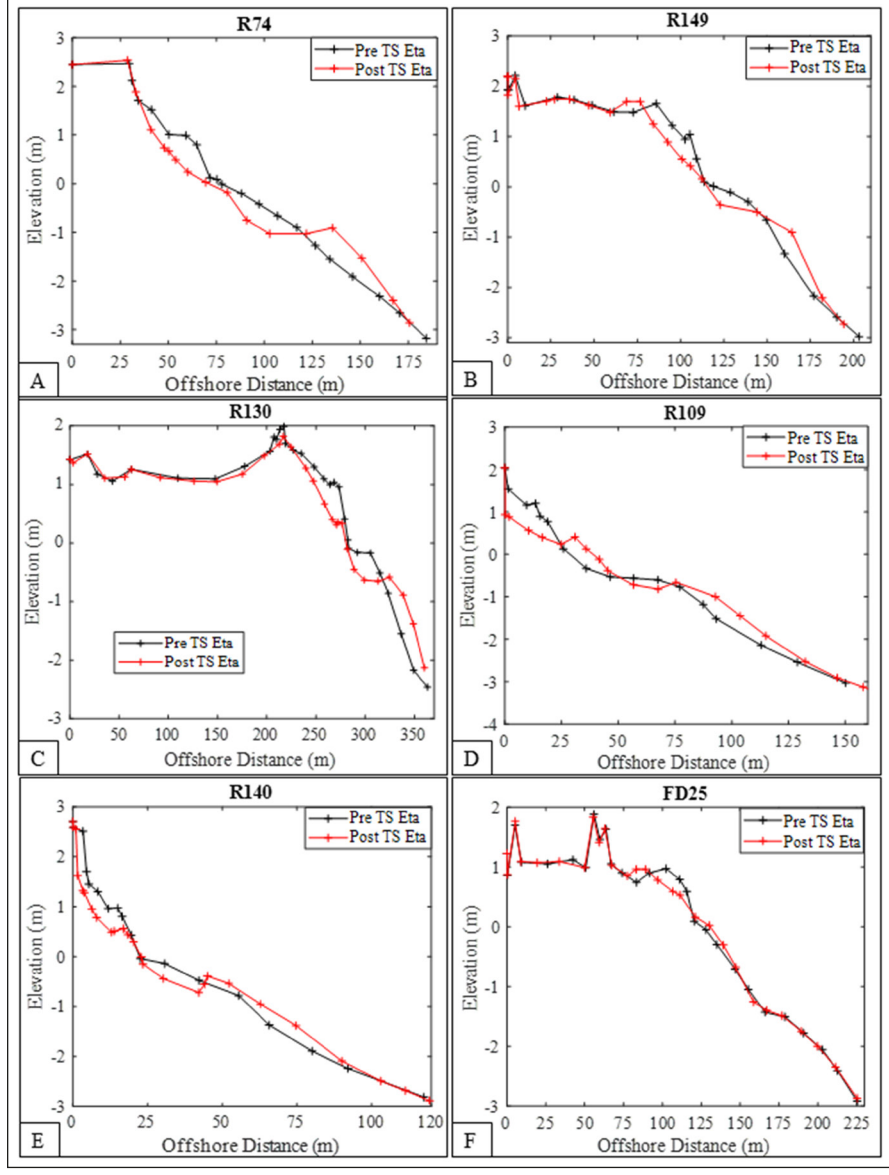


Figure 5. Examples of beach-profile changes induced by TS Eta: A) R74 at northern Sand Key; B) R149 at the middle of Long Key; C) R130 at northern Treasure Island; D) R109 at southern Sand Key; E) R140 at southern Treasure Island; and F) FD25 at southern Mullet Key.

which was defined at the location of the NOAA wave Station 42098; the nearshore storm wave height as computed by the CMS-WAVE model is considerably lower than 2 m (6.6 ft).

### Computation of the Miller and Livermont Storm Erosion Index (SEI)

To calculate the storm erosion potential (SEI), we used the equation, developed by Miller and Livermont (2008).

$$SEI = \sum IEI(t_i) = \sum \{W_*(t_i)[0.068H_b(t_i) + S(t_i)/B + 1.28H_b(t_i)]\}$$
 (1)

where *IEI* refers to Instantaneous Erosion Index. The duration of the storm is accounted for by summing the *IEI* over the period when the storm wave criterion was met. W is the width of the

active surf zone,  $H_{\nu}$ , is the depth limited breaking wave height. In this study, the  $H_{k}$  is determined directly from the CMS-Wave model. S is the water level, which is obtained from the NOAA measured water level at the Clearwater Beach gauge, which is located just to the north of the study area (Figure 1 left panel). It is assumed here that the level of storm surge did not change significantly over a distance of 40 km. B is the berm height, determined from the measured pre-storm beach profile. The width of the active surf zone  $(W_*)$  depends on the breaking wave height  $(H_{i})$ , computed based on Miller and Livermont (2008) as

$$W_* = (h_b/A)^{3/2} (2)$$



Figure 6. Examples of dune erosion and overwash deposit induced by TS Eta.

where A is the sediment scale parameter, which is 0.15 m  $^{1/3}$  for this study area (Wang and Davis 1999). The water depth at the breakpoint  $h_b$  is calculated based on  $H_b$ =0.8 $h_b$ . The time-series of breaking wave height ( $H_b$ ) for the 38 representative beach profile locations were extracted at the seaward slope of sandbar from the modeled wave field for the computation of SEI using Equation (1).

### **RESULTS**

## Hydrodynamic conditions and typical beach-profile changes

The water level variations measured at NOAA Clearwater Beach tide station, illustrate a sustained storm surge above 1.0 m (3.3 ft) for a few hours (Figure 3). The wave conditions were measured at NOAA NDBC Station 42098, about 30 km (19 miles) south of the study area (Figure 1). The high storm waves approached dominantly from the south with the highest measured significant wave height reaching 4.0 m (13.1 ft), and peak wave period reaching 11 s (Figure 3). Driven by the strong southerly wind, a northward flowing longshore current was observed in the field during the storm. In general, TS Eta generated waves that are up to 10 times higher than the average wave conditions along this coast, and with a much longer wave period of roughly 11 s versus the average period of 5 s. The CMS-WAVE model simulated the time-series of wave field when the wave height at the offshore domain boundary was greater than 2.0 m (6.6 ft), defined here as the threshold of storm waves. A snapshot of the modeled wave field at the peak of the storm is illustrated in Figure 4. The wave height along northern Sand Key is greater than that along southern Sand Key, Treasure Island and Long Key. Sheltered by the great Tampa Bay ebb tidal delta, the nearshore wave height along Mullet Key is substantially lower than that along the three barrier islands to the north (Figure 4).

Considerable longshore variations of beach-profile changes were measured. Six representative example beach profiles are shown in Figure 5. In general, sand loss occurred in the dune field, on the dry beach, and in the nearshore zone, while sand gain occurred over the nearshore bar, particularly on the seaward slope of the sandbar. At most of the profile locations, the sand bar was moved offshore by the storm. This general pattern of beach changes is illustrated using profile R74 located on northern Sand Key as an example (Figure 5A). At some beach profile locations, especially those with a wide pre-storm back beach, a storm berm was formed. This is illustrated using profile R149 located on Long Key island as an example (Figure 5B). Part of the back beach gained sand resulting in an overall higher elevation at the storm berm. Substantial erosion typically occurred on the dry beach and in the nearshore area in this case, with part of the eroded sand deposited in the form of a storm berm. For this example (Figure 5B), sand volume gain occurred on the dry beach between 60 m (197 ft) and 80 m (263 ft) (cross-shore distance) due to the washover deposits. Profile R130 located on Treasure Island is another example profile with a wide prestorm back beach. Although considerable erosion occurred at the beach and in the nearshore, the dune field that is quite far from the shoreline was intact due to the protection from the wide pre-storm beach (Figure 5C).

Along sections with a narrow prestorm beach backed by a seawall, severe erosion particularly in terms of the percentage of pre-storm beach width or volume occurred on the dry beach with scour in front of the seawall, exposing the riprap at several locations. In the case of profile R109 (Figure 5D), used here as an example, severe scour occurred along

the exposed seawall, with the entire prestorm dry beach eroded. Along sections with a narrow pre-storm beach, the dune suffered significant erosion, resulting in the formation of a high dune scarp or landward movement of the pre-storm scarp. In the example case of R140 (Figure 5E), where a dune scarp existed before the storm, the scarp became higher and moved landward about 4.0 m (13.1 ft), along with the erosion of the entire prestorm dry beach and severe erosion in the nearshore. The profile FD25 is located on Mullet Key (Figure 5F). As compared to the profiles located on the other barrier islands to the north, the profile FD25 experienced much less erosion, and dune field remained largely unchanged (Figure 5).

### Beach-profile volume changes induced by Tropical Storm Eta

Throughout the four studied barrier islands, sand volume loss in the dune field, i.e. above NAVD88 1.3 m (4.3 ft), is mostly less than 5 m<sup>3</sup>/m (2.0 cy/ft). The high storm waves superimposed on the elevated water level reached the toe of dunes at various places and caused some dune erosion (Figure 6). However, the overall impact to the dune field is not too significant due to the relatively low storm surge of slightly above 1 m (3.3 ft) during a neap tide and a short storm duration. Overwash occurred at a few places on the back beach and in the dune field. Based on the Sallenger (2000) scale, the impact of TS Eta was mostly swash regime (Scale 1) with some collision (Scale 2) regime at places.

The longshore averaged profile volume loss measured above the mean high tide, i.e. sand loss from the dry beach and dune field, at Sand Key, Treasure Island, and Long Key were  $12.9 \text{ m}^3/\text{m}$  (5.1 cy/ft), 13.3 m<sup>3</sup>/m (5.3 cy/ft), and 9.8 m<sup>3</sup>/m (3.9 cy/ft), respectively (Figure 7 A, B, C). A large and highly 3-dimensional swash bar complex (Sandoval 2015) existed at the northern end of the Mullet Key near the Bunces Pass, which has significant influence on the beach-profile changes. It is beyond the scope of this paper to examine beach changes in the close vicinity of tidal inlets. Thus, the beach profiles located at northern Mullet Key were not included in the volume calculations. Seven beach profiles (from FD21 to FD27) located along the middle and southern portion of Mullet Key were included (Figure 7D). The longshore averaged volume loss

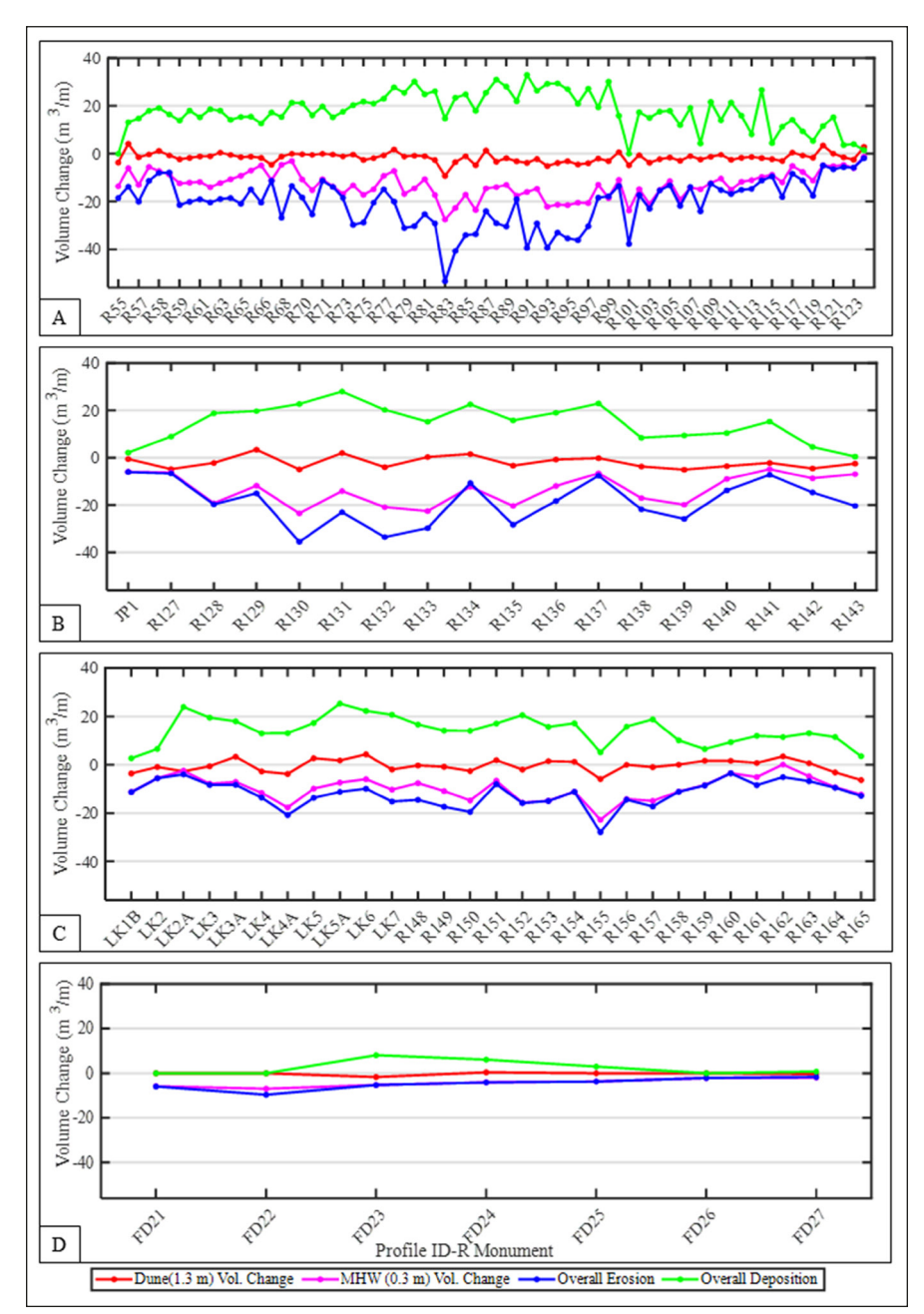


Figure 7. Profile volume change above the dune line, above the mean high tide level, overall erosion and overall deposition on A) Sand Key, B) Treasure Island, C), Long Key, and D) Mullet Key.

above high tide level at these survey lines on Mullet Key is 4.3 m³/m (1.7 cy/ft) (Figure 7D), which is considerably smaller than the volume losses at the three barrier islands to the north. This is related to the considerably lower incident wave along the coast of Mullet Key (Figure 4), due to the wave sheltering by the large Tampa Bay ebb tidal delta for the southerly approaching waves, particularly by the shallow channel margin linear bar along the Tampa Bay main entrance (Figure 1).

The longshore averaged overall sand volume loss from the dune, beach and nearshore exhibits a general southward decreasing trend, with the values at Sand Key, Treasure Island, Long Key and Mullet Key being 20.5 m<sup>3</sup>/m (8.2 cy/ft), 18.7 m<sup>3</sup>/m (7.4 cy/ft),12.0 m<sup>3</sup>/m (4.8 cy/ ft), and 4.7 m<sup>3</sup>/m (1.9 cy/ft), respectively (Figure 7, blue lines). The decreasing trend of overall volume loss is consistent with the decreasing trend of the nearshore wave height along the study area (Figure 4). The highest overall volume loss occurs at profile locations of R81 to R97 (Figure 7A), around the abroad headland of Sand Key and directly to the south, where the nearshore wave is the highest (Figure 4). The overall volume gain mainly at the seaward slope of longshore bar is

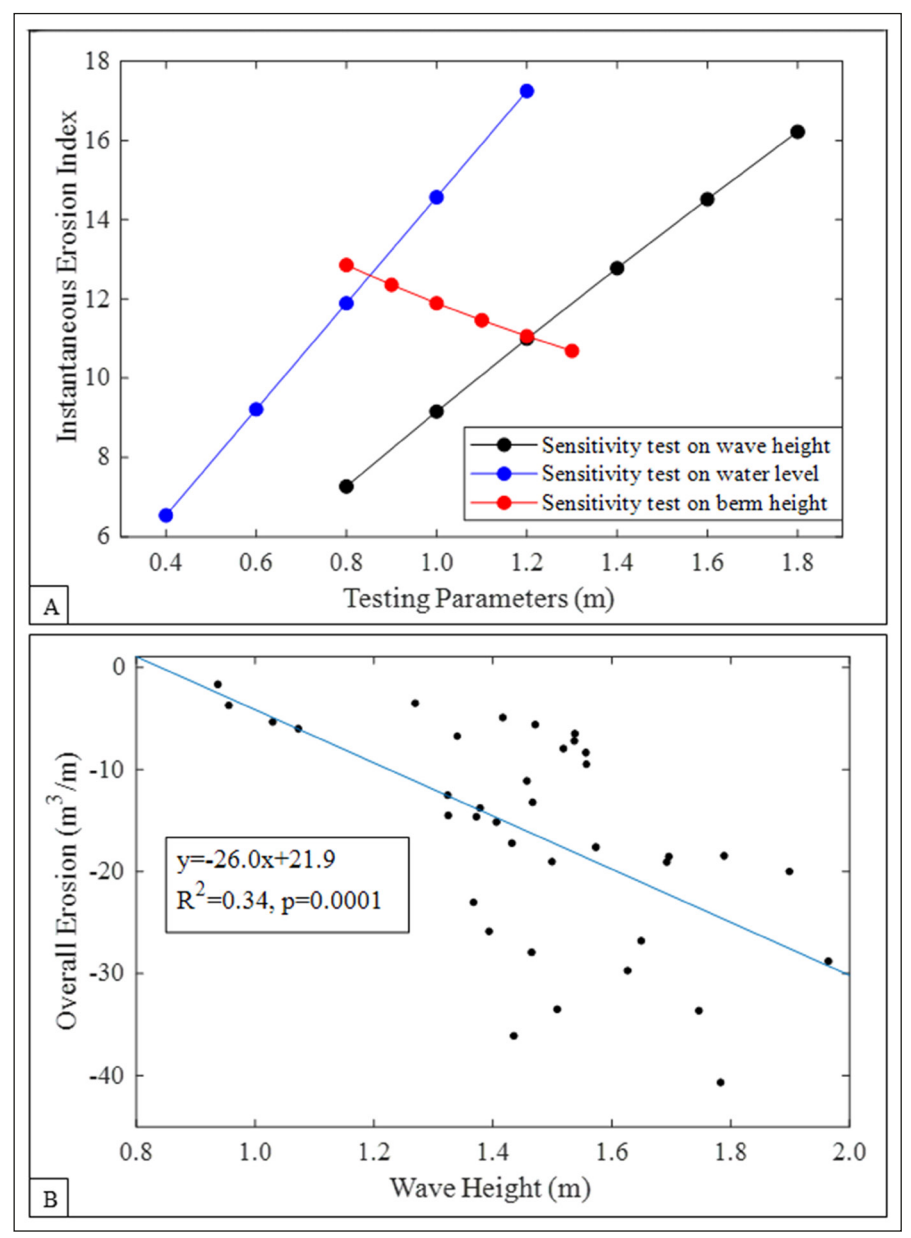


Figure 8. A) Sensitivity tests on the influence of wave height, water level, and berm height. B) A statistically significant correlation exists between the nearshore wave height and overall profile volume loss.

roughly equal to the overall volume loss at the four barrier islands (Figure 7). It is worth noting that for Sand Key the longshore distribution patterns of sand volume loss and sand volume gain are not the same (Figure 7A). The sand volume gain is skewed to the south as compared to the sand volume loss. Similar trend is observed at Treasure Island although to a lesser extent. This southward skew of sand gain may be related to the southward decreasing wave height, although the net longshore transport direction during the storm was towards the north.

### Overall sand volume loss and gain

Almost the entire stretches of Sand Key, Treasure Island, and Long Key suffered dune, dry beach and nearshore erosion, while the nearshore bar, particularly its seaward slope, gained substantial amount of sand (Figure 7A, B, C). Along the 21 km (13 miles) studied section of Sand Key, a total of 35,000 m<sup>3</sup> (46,000 cy) of dune sand was eroded, in addition to 238,200 m3 (311,600 cy) of sand eroded from the dry beach. Substantial erosion also occurred in the nearshore zone. Including the dune, dry beach, and nearshore erosion, the total sand loss along Sand Key amounted to 434,500 m<sup>3</sup> (568,300 cy) with most of the erosion occurring on dry beach (55%). A total sand volume gain of 377,700 m<sup>3</sup> (494,000 cy) was measured in the offshore area, with most of the deposition occurring along the seaward slope of the sand bar (Figure 5). Therefore, about 87% of the sand loss from the dune, dry beach, and nearshorebar can be accounted for by the deposition in the offshore area. The rest of the sand is likely deposited on the ebb shoals.

For Treasure Island, along the 4.8 km (3.0 miles) of the studied section, a total of 9,500 m<sup>3</sup> (12,400 cy) of dune sand loss was measured (Figure 7B). The dry beach lost 60,000 m3 (78,500 cy) of sand. Including the dune, dry beach, and nearshore erosion, the total sand loss along Treasure Island amounted to 96,300 m<sup>3</sup> (126,000 cy), again with most of erosion occurring on the dry beach (62%). Most of the sand was deposited in the offshore area, with a total sand volume gain of 78,200 m3 (102,300 cy). Therefore, about 81% of the sand loss from the dune, dry beach, and nearshore bar can be accounted for by the deposition in the offshore area. The rest of the sand is likely deposited on the ebb shoals, similar to the case at Sand Key.

It is worthy to note that the maximum beach-profile volume loss at Treasure Island is at profile location of R130, with the overall volume loss of 35.5 m³/m (14.2 cy/ft). Profile R130 had a very wide prestorm beach (Figure 5C). On the other hand, the beach profile at R140 with much narrower pre-storm beach width (Figure 5E) experienced less volume loss as induced by TS Eta (Figure 7B). The effect of pre-storm beach widths on the beach-profile volume changes will be discussed in the next section.

Along the 6.3 km (3.9 miles) studied section of Long Key, a total of 1,700 m³ (2,200 cy) of sand loss was measured in the dune field. The dry beach lost 61,300 m³ (80,200 cy) of sand. Including the dune, dry beach, and nearshore erosion, the total sand loss along Long Key amounted to 77,600 m³ (101,500 cy) (Figure 7C), again with most of the sand eroded from the dry beach (79%). Most of the eroded sand was deposited in the offshore area, with a total sand volume gain of 87,300 m³ (114,200 cy), slightly greater than the overall sand loss.

Overall, for the three barrier islands (Sand Key, Treasure Island, and Long Key), a total of 608,300 m³ (795,600 cy) of sand were eroded from the dune field, the dry beach, and the nearshore. About 89% of the eroded sand can be accounted for by the deposition over the nearshore bar, with a total gain of 543,300 m³ (710,600

cy) of sand. It is worth noting that the volume change for Mullet Key is not included here due to its close proximity to the large Tampa Bay ebb delta. As a matter of fact, the entire Mullet Key Island can be viewed as part of the Tampa Bay ebb delta.

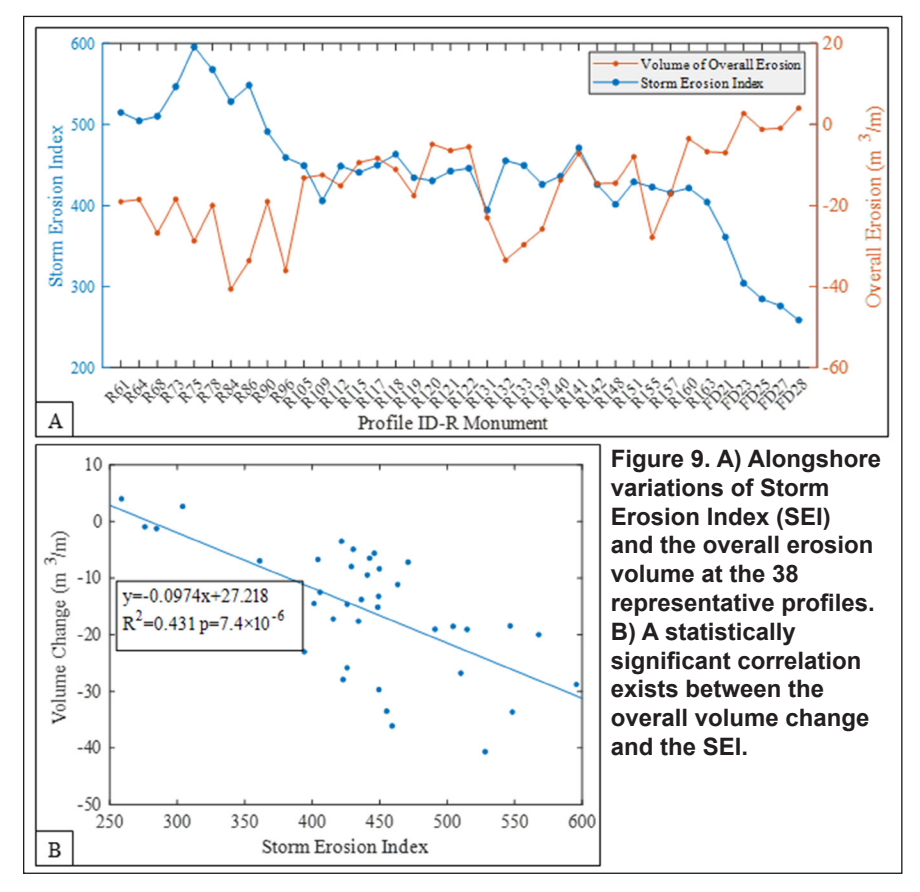
#### **DISCUSSION**

### Reproducing the measured longshore variation using the Miller and Livermont Storm Erosion Index (SEI)

The storm-induced beach profile changes as well as the profile-volume changes demonstrated substantial longshore variations. It would be valuable to beach management, particularly that associated with beach nourishment, if the Miller and Livermont (2008) Storm Erosion Index (SEI) (Eq. 1) can be applied to reproduce the measured longshore variation of beach-profile changes at a finer spatial resolution than previously investigated (Janssen et al. 2019; Lemke and Miller 2020). Based on Equation 1, the breaking wave height  $(H_b)$ , water level (S), and berm height (B) are the main variables for computing the Storm Erosion Index. In order to understand the contributions of these variables to the SEI value, a sensitivity test based on the data from this study was conducted.

Based on the modeled wave field, the breaking wave height  $(H_{\iota})$  at the peak of the TS Eta has a substantial longshore variation ranging from 1.0 m (3.3 ft) to 2.3 m (7.5 ft). The measured pre-storm beach profile demonstrates that the berm height at the study area ranges from 0.8 m (2.6 ft) to 1.3 m (4.3 ft); and the water level with respect to mean sea level ranges from 0.4 m (1.3 ft) to 1.2 m (3.9 ft). Three sensitivity tests were conducted including, 1) with fixed water level (0.8 m or 2.6 ft) and fixed berm height (1 m or 3.3 ft), this test evaluates how the SEI would respond to the changing breaking wave heights; 2) with fixed breaking wave height (1.3 m or 4.3 ft), and fixed water level (0.8 m or 2.6 ft), this test investigates how the SEI would respond to changing berm height, 3) with fixed breaking wave height (1.3 m or 4.3 ft) and berm height (1 m or 3.3 ft), this test examines how the erosion index would respond to the changing water level.

The sensitivity tests suggest that the wave height and water level changes are playing more significant roles in affecting the Instantaneous Erosional Index (IEI) values than that of berm height (Figure



8A). The water level changes are mostly with respect to time. In other words, at the same time, the water level, or storm surge, do not vary too much for a small study area like this one. Thus, the most important spatial variable that cause longshore variation of SEI would be the longshore variation of breaking wave height. A correlation exists ( $R^2$ =0.34) between the longshore variations of breaking wave height at the peak of TS Eta and the corresponding overall profile volume changes (Figure 8B). Although the correlation coefficient is relatively low, the p value (p=0.0001, which is less than 0.05) suggests that the correlation is significant. This suggests the importance of accurately capturing the longshore changes of breaking wave height for the application of the SEI to resolve spatial variations on the order of several hundreds of meters.

The spatial distributions of overall erosion and the SEI are illustrated in Figure 9A at the 38 profile locations. Although not all the profile locations are included in this analysis, the overall trend is represented by these profiles. The calculated storm erosion index shows a general southward decreasing trend from the profiles at northern Sand Key towards Mullet Key, while the corresponding overall erosion volume also show a

southward decreasing trend (Figure 9A). The availability of high-resolution nearshore wave modeling made it possible to calculate nearshore Storm Erosion Index values. A statistically significant correlation exists between the measured longshore variations of volume change and the calculated Storm Erosion Index (Figure 9B). Thus, the SEI is capable of predicting beach-profile erosion at high longshore spatial resolution that is applicable to beach nourishment projects. It is worth noting the  $R^2$  value between the SEI and volume change (0.43) is greater than the  $R^2$  between wave heights and volume change (0.34). This indicates that by including more factors such as storm duration, berm height, and water level, the capability of SEI in predicting storm erosion is improved. The large uncertainty associated with this linear relation indicates that storm-induced beach erosion is complicated, and many factors are at play. Some of the factors are not considered in the SEI.

### Influence of pre-storm beach width on beach profile changes

Based on our field observations during the profile surveys, the pre-storm beach width appeared to play an important role in beach-profile volume changes, as well as percent changes. Since the

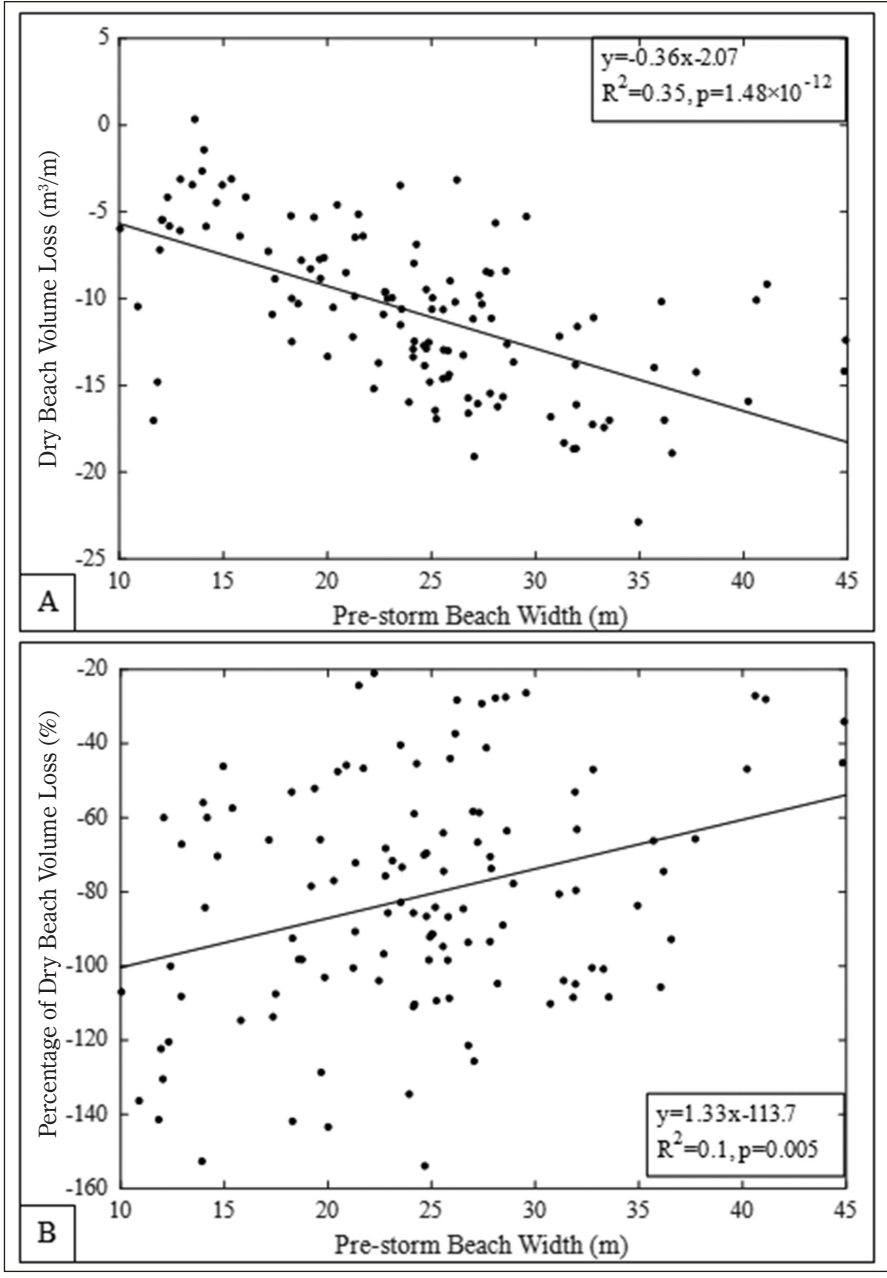


Figure 10. The influence of pre-storm beach width on beach-profile volume changes. A) Relationship between pre-storm beach width and dry beach volume loss. B) Relationship between pre-storm beach width and percentage of dry beach volume loss.

pre-storm beach provides the availability of sand that can be eroded by the storm waves, the wider the pre-storm beach, the larger beach volume loss could occur. On the other hand, narrow pre-storm beach was often completely (or 100%) eroded, leading to dune erosion and infrastructure damage landward, although the profile-volume loss as calculated from the pre- and post-storm profiles can be small. This is illustrated by a statistically significant correlation between pre-storm beach width and beach volume loss (Figure 10A). As indicated by example profiles at Treasure Island, the maximum

beach-profile volume loss occurred at profile R130, where a very wide pre-storm beach existed (Figure 5C). The beach with much narrower pre-storm beach width, e.g. beach profile R140 (Figure 5E), on the other hand, experienced less volume loss (Figure 7B). It is worth noting that the effect of pre-storm beach width on the erosion volume, as illustrated in Figure 10A, may influence the relationship between the erosion volume and the SEI, as shown in Figure 9B.

Furthermore, it is also observed that although more profile volume loss oc-

curred at wider pre-storm beaches, the wide beach provided protection to the dune field and infrastructure landward, resulting in lower percentage of beach volume loss and minimal damage to the features landward (e.g. Figure 5C). In contrast, the narrow pre-storm beach limited the sand volume loss. However, the dune field and infrastructure landward suffered from the storm impact due to the lack of protection by the narrow pre-storm beach (e.g. Figure 5E). Pre-storm beach width and corresponding percentage of beach volume loss (the volume loss measured above the mean high tide line divided by the pre-storm dry beach volume) is plotted in Figure 10B. It is qualitatively apparent that the wider pre-storm beach tends to be associated with smaller percentage of volume loss. For example, when the pre-storm beach width is over 40 m (131 ft), on average about 36% of the dry beach-profile volume was lost at the studied profiles (Figure 10B). In comparison, for the narrow pre-storm beach profiles, considerably higher percentage of volume loss could occur. For example, at the narrow beach with a pre-storm beach width of 12 m (39 ft) at R140 on Treasure Island (Figure 5E), about 130% of beach volume was lost (Figure 10B). It is worthy to note that the greater than 100% dry beach volume loss was caused by the fact that a portion of the dune field was also eroded in addition to the complete erosion of the dry beach. The greater than 100% of dry beach erosion occurred at several profiles with pre-storm beach width less than 30 m (98 ft) (Figure 10B). From a different perspective, the protection offered by wider sections of the beach demonstrates the value of beach nourishment as a coastal protection measure against storm impact. Future study may include the parameter of pre-storm beach width in the SEI to further improve its accuracy in erosion prediction.

### CONCLUSION

Tropical Storm Eta impacted the coast of west-central Florida 11-12 November 2020, and generated high waves superimposed on elevated wave levels for over 20 hours. A total of 148 beach and nearshore profiles, spaced about 300 m (984 ft) apart, were surveyed one to two weeks before and one to eight days after the storm to quantify the beach changes along four barrier islands, including Sand Key, Treasure Island, Long Key and Mullet Key. The high storm waves super-

imposed on elevated water level reached the toe of dunes or seawalls and caused dune erosion and overwash at various places. Along most of the coast, the dune, dry beach and nearshore was eroded and most of the sand was deposited on the seaward slope of the nearshore bar, resulting in a roughly conserved sand volume above closure depth.

The longshore variation of beachprofile volume loss demonstrates an overall southward decreasing trend, mainly due to a southward decreasing nearshore wave height as controlled by the offshore bathymetry and shoreline configurations. The Storm Erosion Index (SEI) developed by Miller and Livermont (2008) captured the longshore variation of beach-profile volume loss reasonably well. The longshore variation of breaking wave height is the dominant factor controlling the longshore change of SEI. Temporal variation of water level also played a significant role, while beach berm elevation was a minor factor.

Although wider beaches tended to experience more volume loss from TS Eta partly due to the availability of sediment, they were effective in protecting the dune and infrastructure landward from storm damage. In contrast, smaller profilevolume loss associated with limited sand availability from narrow beaches do not necessarily relate to less dune and infrastructural damage. Therefore, magnitude of beach-profile volume loss may not be a straightforward indicator of the degree of dune erosion and infrastructure damage. Accurate assessment on storm's severity in terms of erosion potential would benefit beach management especially under the circumstance of increasing storm activities due to climate change.

#### **ACKNOWLEDGEMENTS**

This study was funded by Pinellas County, Florida. Several graduate students from the University of South Florida Coastal Research Laboratory assisted in the field data collection.

### **REFERENCES**

- Beck T.M., and P. Wang, 2019 "Morphodynamics of barrier-inlet systems in the context of regional sediment management, with case studies from west-central Florida, USA." *Ocean and Coastal Management*, 177, 31-51.
- Beck, T.M., Wang, P., Li, H., and W. Wu, 2020. "Sediment bypassing pathways between tidal inlets and adjacent beaches." *J. Coastal Research*, 36, 897-914, https://doi.org/10.2112/JCOASTRES-D-19-00141.1.

- Brutsche K.E., Wang, P., Beck, T.M., Rosati, J.D., and K.R. Legault 2014. "Morphological evolution of a submerged artificial nearshore berm along a low-wave mircotidal coast, Fort Myers Beach, west-central Florida, USA." *Coastal Eng.* 91, 29-44.
- Cheng, J., and P. Wang, 2018. "Dynamic equilibrium of sandbar position and height along a low-wave energy micro-tidal coast." *Continental Shelf Research*, 165, 120-136.
- Cheng, J., and P. Wang, 2019. "Unusual beach changes induced by Hurricane Irma with a negative storm surge and post storm recovery."

  J. Coastal Research, 35, 1185-1199.
- Claudino-Sales, V., Wang, P., and M.H. Horwitz, 2008. "Factors controlling the survival of coastal dunes during multiple hurricane impacts in 2004 and 2005: Santa Rosa barrier island, Florida." *Geomorphology*, 95, 295-315.
- Claudino-Sales, V., Wang, P., and M.H. Horwitz, 2010. "Effect of Hurricane Ivan on coastal dunes of Santa Rosa Barrier Island, Florida: characterized on the basis of pre- and post storm LIDAR surveys." *J. Coastal Research*, 26, 470-484.
- Davis R.A., Wang, P., and B.R. Silverman, 2000. "Comparison of the performance of three adjacent and differently constructed beach nourishment projects on the Gulf Peninsula of Florida." *J. Coastal Research*, 16(2):396-407.
- Davis, R.A., and P. Barnard, 2003. "Morphodynamics of the barrier-inlet system, west-central Florida." *Marine Geology*, 200, 77-101.
- Elko, N.A., and P. Wang, 2007. "Immediate profile and planform evolution of a beach nourishment project with hurricane influence." *Coastal Eng.*, 54(1), 49-66.
- Gibeaut, J.C., and R.A. Davis, 1993. "Statistical geomorphic classification of ebb-tidal deltas along the west-central Florida coast." *J. Coastal Research*, SI 18, 165-184.
- Griggs, G., and K. Patsch, 2019. "Sea-level rise and extreme events where do we go from here?" Shore & Beach, 87(2), 15-28.
- Houston, J.R., 2018. "The economic value of Florida's beaches." *Shore & Beach*, 86(3), 3-13.
- Jose, F., Savarese, M., and A.M. Gross, 2019. "Impact of Hurricane Irma on Keewaydin Island, Southwest Florida coast." *Proc. Coastal Sediments 2019 Conference*, World Scientific, 1142-1151.
- Lin L, Demirbilek, Z., and H. Mase, 2011. "Recent capabilities of CMS-Wave: a coastal wavemodel for inlets and navigation projects." *In:* Rosati, J.D., Wang, P., and T.M. Roberts (eds.), *Proc., Symposium to Honor Dr. Nicholas C.* Kraus. J. Coastal Research, SI 59, 7-14.
- Lemke, L, and J.K. Miller, 2020. "Evaluation of storms through the lens of erosion potential along the New Jersey, USA coast." *Coastal Eng.*, 158, https://doi.org/10.1016/j.coastaleng.2020.103699.
- Janssen, M.S., Lemke, L., and J.K. Miller, 2019. "Application of storm erosion index (SEI) to parameterize spatial storm intensity and impacts from Hurricane Michael." Shore & Beach, 87, 41-50.
- Miller, J.K., and E. Livermont, 2008. "A predictive index for wave and storm surge induced erosion." In: Proc. 31st International Conference on Coastal Eng., 4143-4153. Hamburg, Germany.
- Ojeda, E.; Guillen, J., and F. Ribas, 2011. "Dynamics of single barred embayed beaches." *Marine*

- Geology, 280, 76-90.
- Roberts, T.M., and P. Wang, 2012. "Four-year performance and associated controlling factors of several beach nourishment projects along three adjacent barrier islands, west-central Florida, USA." *Coastal Eng.*, 70, 21-39.
- Roelvink, D., Reniers, A., van Dongeren, A., van Thiel de Vries, J., McCall, R., and J. Lescinski, 2009, "Modelling storm impacts on beaches, dunes and barrier islands." *Coastal Eng.*, 56, 1133-1152.
- Saffir, H.S., 1977. "Design and construction requirements for hurricane resistant construction." American Society of Civil Engineers, Preprint Number 2830, 20p.
- Sallenger, A.H. 2000. "Storm impact scale for barrier islands," *J. Coastal Research*, 16, 890-895.
- Sandoval, E. 2015, Morphodynamics of Mullet Key, West Central Florida. USF graduate theses and dissertations.
- Schott, T., Landsea, C., Hafele, G., Lorens, J., Taylor, A., Thurm, H., Ward, B., Willis, M., and W. Zaleski, 2012. "The Saffir-Simpson hurricane wind scale." NOAA/National Weather Service.
- Simpson, R.H., 1971. "A proposed scale for ranking hurricanes by intensity." *Minutes of the Eighth NOAA, NWS Hurricane Conference*, Miami, Florida.
- Villatoro, M., Silva, R., Méndez, F.J., Zanuttigh, B., Pan, S., Trifonova, E., Losada, I.J., Izaguirre, C., Simmonds, D., Reeve, D.E., Mendoza, E., Martinelli, L., Formentin, S.M., Galiatsatou, P., and P. Eftimova, 2014. "An approach to assess flooding and erosion risk for open beaches in a changing climate." Coastal Eng. 87, 50-76.
- Vidal-Ruiz, J.A., and A. Ruiz de Alegria-Arzaburu, 2019. "Variability of sandbar morphometrics over three seasonal cycles on a single-barred beach." *Geomorphology*, 333, 61-72.
- Wang, P., and R.A. Davis Jr., 1999. "Depth of closure and the equilibrium beach profile — A case study from Sand Key, West-Central Florida." Shore and Beach, 67, 33-42.
- Wang, P., Kirby, J.H., Haber, J.D., Horwitz, M.H., Knorr, P.O., and J.R. Krock, 2006. "Morphological and sedimentological impacts of Hurricane Ivan and immediate post storm beach recovery along the northwestern Florida Barrier-Island Coasts." J. Coastal Research, 22(6), 1382-1402.
- Wang, P., and M.H. Horwitz, 2007. "Erosional and depositional characteristics of regional overwash deposits caused by multiple hurricanes." Sedimentology, 54, 545-564.
- Wang, P., and T.M. Beck, 2012. "Morphodynamics of an anthropogenically altered dual-inlet system: John's Pass and Blind Pass, west-central Florida, USA." *Marine Geology*, 291-294(1), 162-175.
- Wang, P., Adam, J.D., Cheng, J., and M. Vallee, 2020. "Morphological and sedimentological impacts of Hurricane Michael along the northwest Florida coast." *J. Coastal Research*, 36(5), 932-950.
- Wehof, J., Miller, J.K., and J. Engle, 2014. "Application of the storm erosion index (SEI) to three unique storms." *Proc. ICCE 34*, Seoul, Korea. https://doi.org/10.9753/icce.v34.management.39.
- Westfall, Z., 2018. Morphodynamics of Shell key and Mullet Key barrier islands: their origin and development. USF Graduate theses and dissertations.